

Hydrodynamic analysis of self-similar radiative ablation flows

J.-M. Clarisse¹, J.-L. Pfister², S. Gauthier¹, C. Boudesocque-Dubois¹

¹ CEA, DAM, DIF, F-91297 Arpajon, France

² ENS Cachan, F-94235 Cachan, France

Hydrodynamic instabilities, and in particular ablation flow instabilities, are a key and with-standing issue for laser-driven inertial confinement fusion (ICF). In an ongoing effort to obtain a better description of the early-irradiation flow instabilities of an ICF pellet implosion (IPI), a dedicated approach using, as mean flows, self-similar ablative heat-wave solutions of the gas dynamics equations with nonlinear heat conduction [1] in slab symmetry, has been developed and applied to direct laser irradiation configurations [2, 3]. This approach consists in computing, with a spectrally accurate numerical method [4], semi-infinite slab mean flows and their time-dependent linear perturbations. Key features of real ablation flows such as unsteadiness, confinement, compressibility that may be critical to the flow stability, are thus fully and accurately taken into account. Under the assumption of radiative conduction and for positive pressures and radiation fluxes at the slab external boundary, such self-similar solutions can be held as being representative of the ablation of an ICF-pellet shell driven by a gas-filled hohlraum radiation. A logical and preliminary step prior to any hydrodynamic stability study is then to perform a hydrodynamic analysis of such mean flows. In doing so, a framework for analyzing more general (*i.e.* not necessarily self-similar) unsteady ablative mean flows is provided.

Dimensionless equations of motion

The proposed model flow considers the motion of an inviscid, heat-conducting fluid with a polytropic equation of state, $p = R\rho T$, $\mathcal{E} = RT/(\gamma - 1)$, and a nonlinear heat conductivity of the form $\kappa = \kappa_0(\rho_0/\rho)^\mu(T/T_0)^\nu$, $\kappa_0 > 0$, $\mu \geq 0$, $\nu > 0$, where ρ_0 and T_0 are homogenization constants. The fluid which is initially at rest, of uniform finite density ρ_I , and occupying the half-space $x \geq 0$, is set into motion by time-increasing pressure and heat flux applied at its external boundary surface Γ . Relying on the physical governing parameters γ , R , κ_0 , ρ_I , characteristic boundary pressure p_Γ and heat flux φ_Γ , supplemented by a reference time t_c , two dimensionless formulations of the equations of motion in Lagrangian coordinates are proposed:

($\mathcal{B}_p, \mathcal{B}_\varphi$)-formulation [2]

($\mathcal{M}, \mathcal{P}_e$)-formulation

$$\left\{ \begin{array}{l} \partial_{\bar{t}}[1/\bar{\rho}] - \partial_{\bar{m}}\bar{v}_x = 0, \quad \partial_{\bar{t}}\bar{v}_x + \partial_{\bar{m}}\bar{p} = 0, \\ \partial_{\bar{t}}\left[\frac{1}{2}\bar{v}_x^2 + \frac{1}{\gamma-1}\bar{T}\right] + \partial_{\bar{m}}[\bar{p}\bar{v}_x + \bar{\varphi}_x] = 0, \\ \bar{\varphi}_x = -\bar{\rho}\bar{\kappa}\partial_{\bar{m}}\bar{T}, \end{array} \right. \quad \left\{ \begin{array}{l} \partial_{\bar{t}}[1/\bar{\rho}] - \partial_{\bar{m}}\bar{v}_x = 0, \quad \partial_{\bar{t}}\bar{v}_x + \frac{1}{\gamma\mathcal{M}^2}\partial_{\bar{m}}\bar{p} = 0, \\ \partial_{\bar{t}}\left[\frac{1}{2}\bar{v}_x^2 + \frac{1}{\gamma\mathcal{M}^2}\frac{1}{\gamma-1}\bar{T}\right] + \frac{1}{\gamma\mathcal{M}^2}\partial_{\bar{m}}[\bar{p}\bar{v}_x + \bar{\varphi}_x] = 0, \\ \bar{\varphi}_x = -\frac{\gamma}{\gamma-1}\frac{1}{\mathcal{P}_e}\bar{\rho}\bar{\kappa}\partial_{\bar{m}}\bar{T}, \end{array} \right.$$

with $\bar{p} = \bar{\rho}\bar{T}$ and $\bar{\kappa} = \bar{\rho}^{-\mu}\bar{T}^\nu$, and where \bar{m} is such that $d\bar{m} = \bar{\rho}d\bar{x}$. Driving dimensionless parameters, apart from γ , are ascribed with the former formulation to the sole boundary condition parameters \mathcal{B}_p and \mathcal{B}_φ (cf. Tab. 1), while they are, with the latter, enmeshed in the governing equations under the form of Mach and Péclet number scales \mathcal{M} and \mathcal{Pe} . For initial and bound-

	$\bar{\rho}(\bar{m}, 0)$	$\bar{v}_x(\bar{m}, 0)$	$\bar{T}(\bar{m}, 0)$	$\bar{p}(0, \bar{t})$	$\bar{\varphi}_x(0, \bar{t})$
$(\mathcal{B}_p, \mathcal{B}_\varphi)$	1	0	0	$\mathcal{B}_p \bar{t}^{2(\alpha-1)}$	$\mathcal{B}_\varphi \bar{t}^{3(\alpha-1)}$
$(\mathcal{M}, \mathcal{Pe})$	1	0	0	$\bar{t}^{2(\alpha-1)}$	$\bar{t}^{3(\alpha-1)}$

Table 1: Invariant-density self-similar solutions. Initial and boundary conditions.

ary conditions compatible with a reduction of variables (Tab. 1), these formulations lead to two complete classifications of self-similar solutions (cf. Tab. 2).

\mathcal{B}_p	\mathcal{B}_φ	\mathcal{M}^2	\mathcal{Pe}
$(\gamma-1)\gamma^{-2}\mathcal{Pe}\mathcal{M}^{-2}$	$(\gamma-1)^{3/2}\gamma^{-5/2}\mathcal{Pe}^{3/2}\mathcal{M}^{-2}$	$\gamma^{-1}\mathcal{B}_\varphi^2\mathcal{B}_p^{-3}$	$\gamma(\gamma-1)^{-1}\mathcal{B}_\varphi^2\mathcal{B}_p^{-2}$

Table 2: Relations between the driving parameters $(\mathcal{B}_p, \mathcal{B}_\varphi)$ and $(\mathcal{M}, \mathcal{Pe})$.

Invariant-density self-similar radiative ablation flows

Self-similar solutions leaving invariant the flow density correspond to the similarity exponent definition $\alpha = (2\nu - 1)/2(\nu - 1)$ and the similarity laws of Tab. 3, the systems of PDEs being replaced by systems of ODEs for the flow reduced variables, with initial and boundary conditions of Tab. 1 being transformed, respectively, into boundary conditions at $\xi = +\infty$ and at $\xi = 0$ [2]. For sufficiently low values of the external boundary heat flux, the heated fluid

\bar{m}	$\bar{\rho}(\bar{m}, \bar{t})$	$\bar{v}_x(\bar{m}, \bar{t})$	$\bar{T}(\bar{m}, \bar{t})$	$\bar{p}(\bar{m}, \bar{t})$	$\bar{x}(\bar{m}, \bar{t})$
$\bar{t}^\alpha \xi$	$G(\xi)$	$\bar{t}^{\alpha-1}V(\xi)$	$\bar{t}^{2(\alpha-1)}\Theta(\xi)$	$\bar{t}^{2(\alpha-1)}P(\xi)$	$\bar{t}^\alpha X(\xi) = \bar{t}^\alpha [V(\xi)/\alpha + \xi/G(\xi)]$

Table 3: Invariant-density self-similar solutions. Dependent/independent-variable reduction.

region may be considered to be bounded by a non-isothermal shock-wave discontinuity [1, § C] and the boundary conditions at $\xi = +\infty$ replaced by the relevant Rankine–Hugoniot jump relations at the shock-front location (e.g. [2]). Self-similar radiative ablation flows within this bounding shock-wave approximation have been investigated — for a monatomic gas ($\gamma = 5/3$) and the fully ionized gas model of Kramers ($\mu = 2$, $\nu = 13/2$) — by means of an extensive exploration of the space of parameters $(\mathcal{B}_p, \mathcal{B}_\varphi)$ for solutions computable with the numerical method detailed in [4]. A set of 631 ablative solutions, presenting a large variety of spatial pro-

files (Figs. 1a, c, e, g) and including a solution extrapolated from an IPI simulation with an ICF hydrodynamics code (IPI-like flow), has thus been obtained.

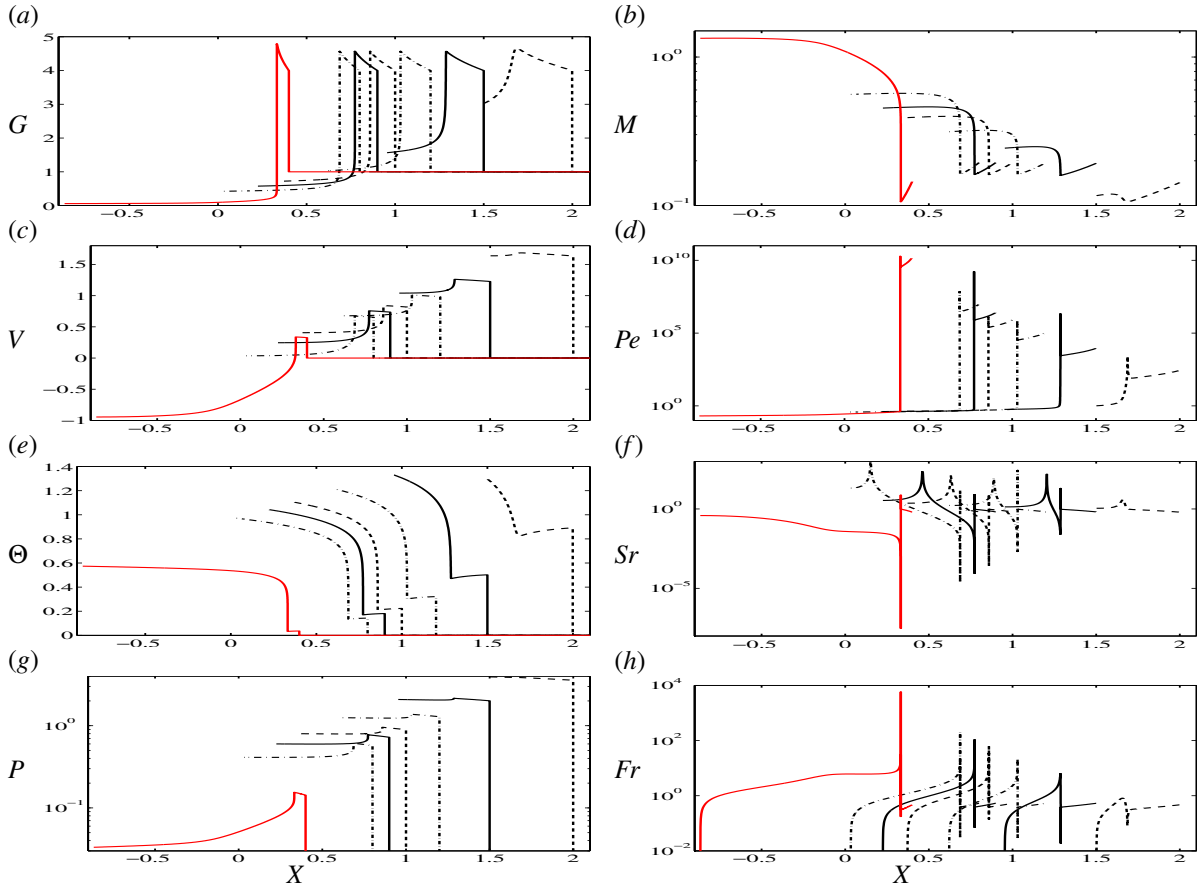


Figure 1: Reduced flow variables (a, c, e, g) and hydrodynamic characteristic numbers (b, d, f, h) vs the reduced coordinate X (Tab. 3), for a particular flow sample (IPI-like flow in red).

Hydrodynamic analysis

The analysis of these ablative flows has been performed in the reference frame of the ablation front (af) — here ascribed to be the locus of the minimum temperature-gradient length, $\ell_T = \min_x \ell_{\nabla T}$ — leading to the definition of local Mach, Péclet, stratification and Froude numbers in terms of the fluid velocity relative to the ablation front v'_x , the ablation-front acceleration a_{af}^e , and proper local gradient lengths (Tab. 4). Completed by the flow-region rela-

	Mach	Péclet	stratification	Froude
flow analysis	$M = \frac{ v'_x }{\sqrt{\gamma p/\rho}}$	$Pe = \frac{ v'_x \ell_{\nabla T}}{\kappa / \rho R}$	$Sr = \frac{\ell_{\nabla p} a_{\text{af}}^e }{p / \rho}$	$Fr = \frac{ v'_x }{\sqrt{ a_{\text{af}}^e \ell_{\nabla v'}}}$
LM criteria	$\gamma M^2 \ll 1$	$\frac{\gamma^2}{\gamma-1} \frac{M^2}{Pe} \ll 1$	$Sr' = \frac{\ell_{\nabla v'} a_{\text{af}}^e }{p / \rho}$	$\frac{\gamma M^2}{Fr^2} (= Sr') \ll 1$

Table 4: Hydrodynamic characteristic number definitions and LM approximation criteria.

tive lengths $\ell_{\text{cond}}/\ell_{\text{tot}}$ (conduction region), ℓ_T/ℓ_{tot} (ablation-front stiffness), and $(1 - \ell_{\text{cond}}/\ell_{\text{tot}})$

(compressed-fluid region), this analysis yields a global and detailed description of the flow hydrodynamic features. For example, strong compressibility effects — fast expansions of the heated fluid ($\ell_{\text{cond}}/\ell_{\text{tot}} \approx 1$, Figs. 2a, b), isentropic Chapman–Jouguet (CJ) points ($M = 1$, Figs. 1b and 2c, d), ablation fronts with high stiffnesses and strong dominance of pressure gradients over inertial forces ($Sr_{\text{af}} \ll 1$, Fig. 1f) — are evidenced for sufficiently large values of the Péclet scale $\mathcal{P}e$ ($\propto \mathcal{B}_{\phi}^2/\mathcal{B}_p^2$), and in particular for the IPI-like flow. Regarding the

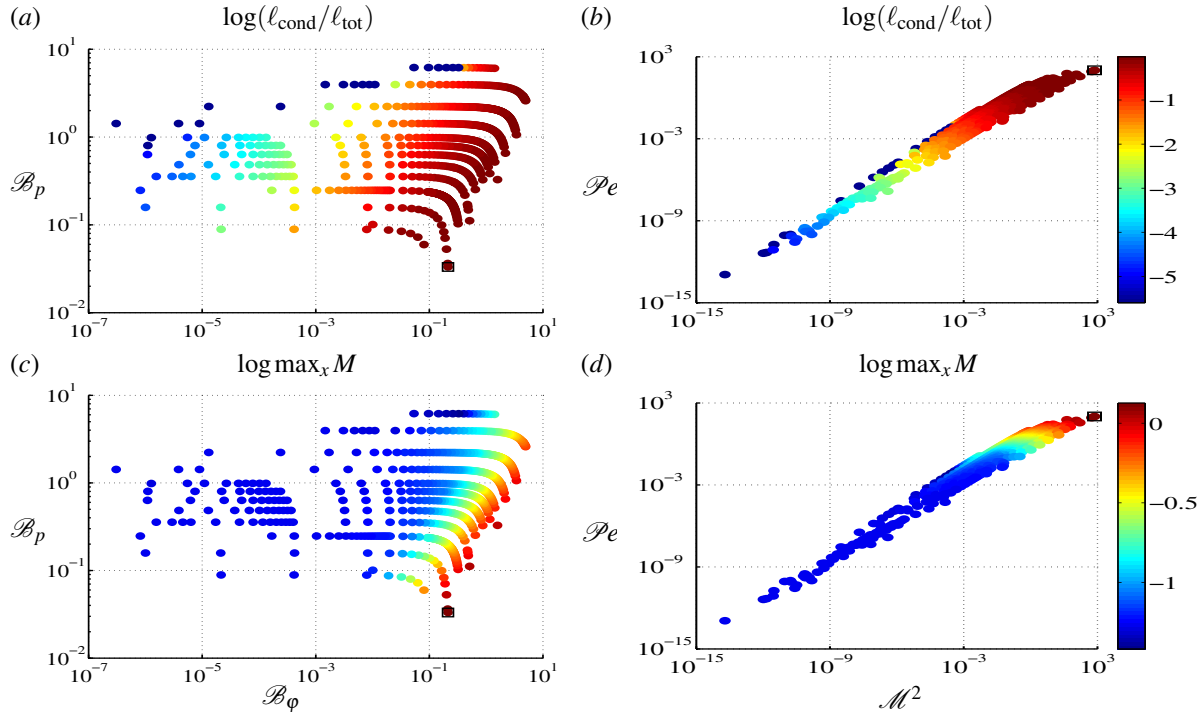


Figure 2: Radiative self-similar flow. Hydrodynamic characteristic numbers (IPI-like flow \square).

low-Mach-number (LM) approximation commonly used in ablative Rayleigh–Taylor instability modeling, none of the flows satisfies the Froude criterion $\gamma M^2/Fr^2$ ($= Sr'$) $\ll 1$ (see Tab. 4) in the vicinity of the external surface and of the ablation front (Fig. 1h), while flows with CJ points obviously do not fulfill the low-Mach criterion over part of their conduction region (Fig. 1b). For arbitrary time-dependent flows, the same set of characteristic numbers is equally relevant, the corresponding analysis having to be performed repeatedly over time.

References

- [1] R. Marshak, Phys. Fluids **1**, 24 (1958)
- [2] C. Boudesocque-Dubois, S. Gauthier and J.-M. Clarisse, J. Fluid Mech. **603**, 151 (2008)
- [3] J.-M. Clarisse, C. Boudesocque-Dubois and S. Gauthier, J. Fluid Mech. **609**, 1 (2008)
- [4] C. Boudesocque-Dubois, V. Lombard, S. Gauthier and J.-M. Clarisse, J. Comp. Phys. **235**, 723 (2013)